NON-LINEAR BEAM TRANSPORT OPTICS FOR A LASER WAKEFIELD ACCELERATOR*

C. Widmann[†][1], V. Afonso Rodriguez[1], A. Bernhard[1], N. Braun[1], B. Härer[1],
O. Jäckel[3], M. Nicolai[2], P. Peiffer[1], M. Reuter[3], T. Rinck[2], R. Rossmanith[1],
A. Sävert[2], M. Scheer[4], W. Werner[1], T. Baumbach[1], M. C. Kaluza[2,3],

[1]Karlsruhe Institute of Technology (KIT), Germany   [2]Friedrich Schiller University Jena, Germany
[3]Helmholtz Institute Jena, Germany   [4]Helmholtz Zentrum Berlin (HZB), Germany

Abstract

The transport and matching of electron beams generated by a Laser Wakefield Accelerator (LWFA) is a major challenge due to their large energy spread and divergence. The divergence in the range of one milli-radian at energies of some 100 MeV calls for strong focusing magnets. At the same time a chromatic correction of the magnets is needed due to the relative energy spread of a few percent.

This contribution discusses in particular the layout of the beam transport optics for a diagnostic beam-line at the LWFA using the JETI laser in Jena, Germany. The aim of this optics is to match the β-functions and the non-zero dispersion to the x-dependent flux density amplitude of a transverse gradient undulator such that monochromatic undulator radiation is generated despite the large energy spread.

The transport line is realized as a dogleg chicane involving several strong focusing quadrupoles. The chromatic error is compensated by additional sextupoles. To keep the setup as compact as possible the magnets are designed as combined function magnets. In this contribution the design and optimization of the transport optics, as well as their realization are presented.

INTRODUCTION

A combination of a LWFA with a short period undulator is a promising candidate for a compact light source. With accelerating gradients up to some 100 GV/m and a short acceleration length of some millimeters the accelerator itself is quite compact.

However, a major drawback is the large relative energy spread of some percent that deteriorates the monochromaticity and intensity of undulator radiation. To overcome these problems an alternative concept was proposed [1, 2]: The bunch is energetically dispersed in one spatial direction and matched to the magnetic field amplitude of a transverse gradient undulator, so that all electrons of different energies emit radiation at the same wavelength.

This concept will be applied to the LWFA in Jena to design a diagnostic beamline: Monochromatic undulator radiation will be used to measure the transverse beam size and emittance of the bunch. A sketch of the setup is shown in Fig. 1. The electron bunch is dispersed in a dogleg chicane consisting of two dipoles and several focusing mag-
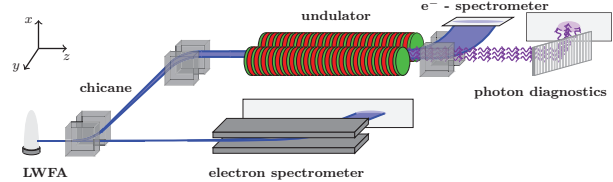

Figure 1: Sketch of the setup: The electron bunch is dispersed in the chicane and by using several focusing magnets matched to the field amplitude of a cylindrical undulator, where monochromatic undulator radiation is generated. The radiation will be used to measure the transversal bunch size and emittance.

nets and matched to the field of a cylindrical undulator. Assuming the bunch consists of a number of monoenergetic beamlets, the position and beam parameters of each beamlet have to fulfill the requirements imposed by the undulator. After traversing the undulator, the bunch is deflected to an electron spectrometer. The spectrum and source properties of the undulator radiation will be characterized.

The design of the superconducting, cylindrical undulator has been discussed in a previous publication [3]. The undulator consists basically of two cylindrical coils with $N = 100$ periods of length $\lambda_u = 10.5$ mm, i.e. the natural bandwidth of the undulator radiation of a monoenergetic bunch would be $\Delta\lambda/\lambda = 1/N = 1\%$. The goal of the experiment is to achieve this bandwidth for all electrons in the range of 120 MeV $\pm 10\%$.

As the position of the monoenergetic beamlets is matched to the field gradient of the undulator, the electrons pass the undulator slightly off center in x. The optimized field amplitude and the position of several monoenergetic beamlets are shown in Fig. 2. For the beamlet of 120 MeV the gap is 2.4 mm. The expected radiation wavelength λ of about 142 nm is estimated using the undulator equation

$$\lambda = \frac{\lambda_u}{2\gamma_e(x)} \left(1 + \frac{K(x)^2}{2} \right) \qquad (1)$$

with the relativistic parameter γ_e. The undulator parameter $K(x) = \frac{2\pi e}{m_e c} \lambda_u \tilde{B}_y(x)$ depends on the magnetic field amplitude $\tilde{B}_y$ at the entrance position x of each energy.

The beam parameters to be matched by the beam transport system are determined by these special undulator properties, as will be discussed in the following sections.

05 Beam Dynamics and Electromagnetic Fields

D01 Beam Optics - Lattices, Correction Schemes, Transport

(a) cross-section of the undulator   (b) magnetic field amplitude $\tilde{B}_y(x)$
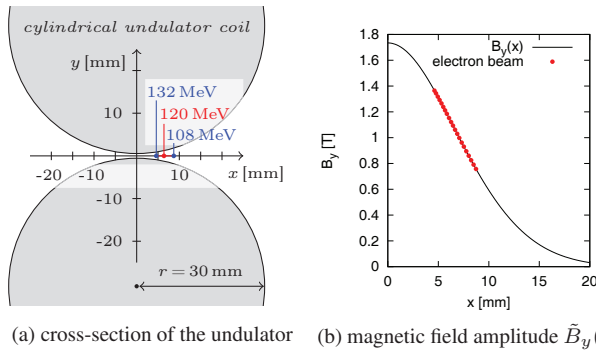
Figure 2: (a) Cross-section of the undulator with the position of three monoenergetic beamlets. (b) Magnetic field amplitude $\tilde{B}_y(x)$ and the position of the beamlets.

BEAM DYNAMICS IN THE UNDULATOR

The cylindrical undulator requires parameters that differ from the beam parameters usually required in a planar undulator. In the deflection plane (x, z) a small displacement of an electron trajectory in x results in a local change of the magnetic field amplitude and therefore in a shift of the radiated wavelength. Thus each monoenergetic beamlet has to be as small as possible along the undulator to preserve the radiation's monochromaticity. In the (y, z) plane the small gap of the undulator is the limiting parameter. Therefore the size of the beamlets should also be as small as possible.

To find the optimal beam parameters at the entrance of the undulator analytical calculations were performed considering the focusing and defocusing effects of the undulator fields in linear approximation.

Non-deflection plane (y, z) Perpendicular to the deflection plane the focusing is described similar to a planar undulator, where the longitudinal fields between two poles focus the beam. This approximation holds as the field component B_x can be neglected in the area of the beam. The average focusing parameter integrated over one period λ_u is given by (see e.g. [4])

$$\hat{k} = \left(\frac{e}{\gamma_e m_0 c}\right)^2 \frac{1}{\lambda_u} \int_0^{\lambda_u} B_y(z)^2 dz. \qquad (2)$$

The focusing parameter $\hat{k}$ is inserted into the transfer matrices for a focusing quadrupole of length $N \cdot \lambda_u \approx 1.10$ m, i.e. the length of the undulator, to transform the twiss parameters β, α and $\gamma = \frac{1+\alpha^2}{\beta}$ through the undulator. The smallest beam size is achieved for a constant β along the undulator, i.e. at the entrance of the undulator $\alpha_0 = 0$ and $\beta_0 = \beta_{\text{exit}}$. The resulting equation can be solved for β_0. Different γ_e and $\tilde{B}_y$ for each electron energy lead to different values of β_0. The values for the minimum, central and maximum energy are listed in Tab. 1. As target parameter for all energies $\beta_0 = 0.6$ m is chosen as a compromise. The resulting β-functions are shown in Fig. 3b.

Deflection plane (x, z) The gradient $\frac{d\tilde{B}_y}{dx}$ of the field amplitude in the cylindrical undulator is approximately constant near the reference trajectory for each energy. The field amplitude can be written as $\tilde{B}_y = \tilde{B}_{y0} + \frac{d\tilde{B}_y}{dx}\Delta x$

Table 1: Field amplitude $\tilde{B}_y$, maximum field gradient $\frac{d\tilde{B}_y}{dx}$ and initial values β_0 with $\alpha_0 = 0$ for constant resp. periodic β-functions along the undulator.

	$\tilde{B}_y$	$\beta_y = $ const.	$\left\|\frac{d\tilde{B}_y}{dx}\right\|$	β_x period.
108 MeV	0.76 T	0.68 m	137 T/m	2.22 m
120 MeV	1.09 T	0.52 m	152 T/m	2.22 m
132 MeV	1.37 T	0.46 m	140 T/m	2.66 m

where $\tilde{B}_{y0}$ is the magnetic field amplitude at the according reference trajectory. The field gradient causes a ponderomotive drift of the trajectories, which is basically compensated by a superposed, constant correction field B_y^{corr} (for details see [3]). Here we assume an ideal correction of this drift and do not further consider it. The gradient for a sinusoidal field along the trajectory is given by $\frac{dB_y}{dx}(z) \approx \frac{d\tilde{B}_y}{dx}\sin\left(\frac{2\pi z}{\lambda_u}\right) = g(z)$, i.e. the focusing can be described by the matrix of a focusing resp. defocusing quadrupole with $k = \frac{eg}{\gamma_e m_0 c}$. The whole undulator is therefore a series of alternating focusing and defocusing sections. Again by solving the transfer equation of the twiss parameters for $\alpha_0 = 0$ and $\beta_0 = \beta_{\text{exit}}$ a solution for a periodic β-function can be found. However, the resulting values listed in Tab. 1 are too large. As the focusing is weak, the initial conditions of a drift space with a beam waist in the center of the undulator and $\beta = L/2 \approx 0.5$ m results in the smallest beamsize. The β-function along the undulator in this case is shown in Fig. 3a.
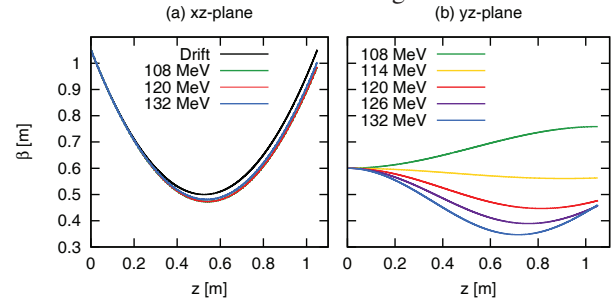

(a) xz-plane   (b) yz-plane

Figure 3: Smallest β-functions along the undulator for both transversal planes considering the focusing of the undulator field.

To verify the analytical calculations, tracking simulations were performed using the FEM undulator model. The results of these calculations differ less than 5 % from the analytical calculations, so the analytical model can be used for a 1st−order approximation.

BEAM TRANSPORT SYSTEM

The initial transversal distribution of the electron bunch is assumed to be gaussian with a source size $\sigma_{x,y} = 10\,\mu$m and divergence $\sigma_{x',y'} = 1$ mrad. Assuming a beam waist at the exit of the LWFA, the geometrical emittance ϵ is 10 nm rad and the initial twiss parameters are $\beta = 0.01$ m and $\alpha = 0$.

The beam transport system consists of two dipole magnets ($l_z = 50$ mm, $B_{y,max} = 0.46$ T) and seven combined

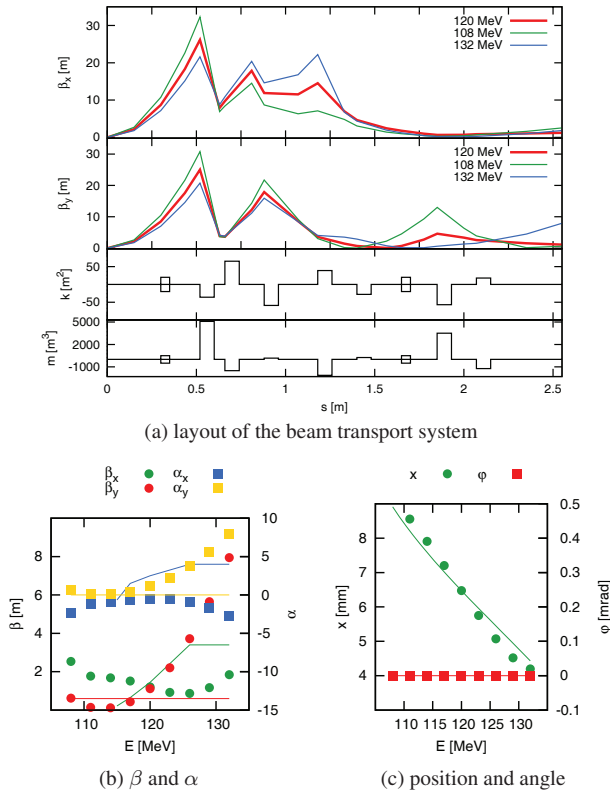05 Beam Dynamics and Electromagnetic Fields

D01 Beam Optics - Lattices, Correction Schemes, Transport

(a) layout of the beam transport system

(b) β and α (c) position and angle

Figure 4: (a) Beam transport optics: β functions, quadrupole component k and sextupole component m of the magnets. (b) Beam parameters and (c) entrance position and angle achieved (dots) at the undulator in the optimization and new target parameters (lines).

quadrupole-sextupole magnets ($l_z = 80\,\mathrm{mm}$). The simulations of the optics were performed with the Polymorphic Tracking Code (PTC) in MAD-X [6] using as target parameters the values found in the previous section, a splitting $\Delta x = x\,(108\,\mathrm{MeV}) - x\,(132\,\mathrm{MeV}) = 4\,\mathrm{mm}$ and $\varphi = \frac{dx(E)}{dz} = 0$, i.e. parallel beamlets inside the undulator. The quadrupole and sextupole strenghts were optimized using the downhill simplex algorithm and the monte carlo method.

The result is shown in Fig. 4a, the parameters achieved for the different energies are shown in Fig. 4b and c. Solutions for focusing optics with chromatic correction for an energy band of 108 MeV to 132 MeV were found. However, the achieved results still need to be improved to generate monochromatic undulator radiation. Further optimizations must be based on simulations of the radiation fields.

SIMULATION OF RADIATION FIELDS

The figure of merit to determine the target parameters for the undulator is the radiation field emitted by the electrons. Therefore simulations of trajectories and radiation fields with *WAVE* [5] were performed using a 3D field map of an ideal cylindrical undulator model as input.

Starting positions $x(E)$ Optimizing the starting positions with Eq. 1 neglects the small drift of the trajectories, which is not fully corrected by the correction field B_y^{corr}
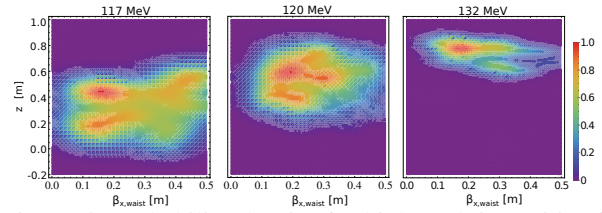

Figure 5: Probability density for high peak intensities for different values of $\beta_{x,\mathrm{waist}}$ at the beam waist and different positions of the beam waist along the undulator (entrance at $z = 0$).

mentioned above. The drift is less than 0.1 mm, but has a significant influence on the wavelength of the radiation emitted by a single electron for each energy. By reoptimizing $x(E)$ using radiation fields simulations the bandwidth $\frac{\Delta\lambda}{\lambda}$ is reduced to 1.0 %.

Twiss parameters of the beamlets   To optimize the beam parameters inside the undulator in the (x, z) plane the value of $\beta_{x,\mathrm{waist}}$ at the beam waist and the position of the beam waist were varied. A bunch of 100 electrons with random initial conditions was used to simulate the spectrum. The probability density for high peak intensities is shown in Fig. 5 for three energies. In all cases the optimal value for $\beta_{x,\mathrm{waist}}$ is around 0.2 m, the optimal position of the waist varies. For 120 MeV it is exactly in the center of the undulator, for 117 MeV and 132 MeV shifted to the entrance or exit, respectively.

In the (y, z) plane, a variation of the initial β has little influence on the peak intensity as the focusing forces of the undulator field generally keep β small. The small undulator gap remains the limiting factor.

The new target values resulting from the radiation field simulations are shown in Fig. 4b and 4c. They will be considered in the reoptimization of the beam optics.

CONCLUSION

A careful analysis of the beam dynamics inside a transverse-gradient undulator leads to target parameters for matching the beam transport optics to the undulator. A first optimization of the focusing optics with strong chromatic correction for transporting and matching electrons in an energy band of 120 MeV ± 10 % was carried out. Based on radiation field simulations, the target parameters required by the undulator were redefined. The next step is to further optimize the beam transport optics with respect to these new target parameters.

REFERENCES

[1] G. Fuchert et al., NIM A, vol. 672, 33-37 (2012).

[2] T. I. Smith. et al., J. Appl. Phys., vol. 50, 4580 (1979).

[3] V. Afonso Rodriguez et al., IEEE Transactions on Appl. Supercond., vol. 23(3), 4101505 (2013).

[4] J. A. Clarke, The Science and Technology of Undulators and Wigglers, Oxford Science Publications (2004).

[5] M. Scheer, Proceedings of the ICAP'12, TUACC2 (2012).

[6] E. Forest et al., KEK-Report, CERN-SL-2002-044 (2002).